NANO · MICRO small
www.small-journal.com

Combining Whispering-Gallery Mode Optical Biosensors with Microfluidics for Real-Time Detection of Protein Secretion from Living Cells in Complex Media

Ying-Jen Chen, Ulrike Schoeler, Chung-Hsuan (Benjamin) Huang, and Frank Vollmer**

The noninvasive monitoring of protein secretion of cells responding to drug treatment is an effective and essential tool in latest drug development and for cytotoxicity assays. In this work, a surface functionalization method is demonstrated for specific detection of protein released from cells and a platform that integrates highly sensitive optical devices, called whispering-gallery mode biosensors, with precise microfluidics control to achieve label-free and real-time detection. Cell biomarker release is measured in real time and with nanomolar sensitivity. The surface functionalization method allows for antibodies to be immobilized on the surface for specific detection, while the microfluidics system enables detection in a continuous flow with a negligible compromise between sensitivity and flow control over stabilization and mixing. Cytochrome c detection is used to illustrate the merits of the system. Jurkat cells are treated with the toxin staurosporine to trigger cell apoptosis and cytochrome c released into the cell culture medium is monitored via the newly invented optical microfluidic platform.

1. Introduction

The study of cell behavior in response to various stimuli has applications in a wide variety of fields ranging from basic biological studies to drug discovery. Quantitative analysis of intracellular components is commonly investigated using invasive methods that lyse or permeabilize cells.[1] Consequently, these assays require the perturbation of cell cultures or even the harvesting and destruction of cells, all of which prevent quantitative real-time monitoring of apoptotic cells responses within live cell cultures. The specific detection of markers (e.g., cytochrome c and active caspase-3) indicative of apoptosis further requires labeling,[2] protein purification procedures, or cell staining.[3] In whispering-gallery mode (WGM) sensing on the other hand, no labeling of the protein with a reporter enzyme or fluorophore is required. Instead, the WGM sensor surface is modified with a detection antibody to achieve label-free and specific protein sensing.[3]

The noninvasive and real-time investigation of intact and nonlabeled cell cultures is of great importance for determining the onset of cell death and understanding mechanisms that trigger apoptosis.[4] Tracking the complex response kinetics of cells thereby requires the noninvasive and real-time monitoring of extracellular markers; however, due to the insufficient sensitivity of common methods, it is quite challenging to track low concentration of protein release to the cell culture medium without fluorescence labeling. Optical-based biosensors are particularly adept at this task as they specifically detect biomolecules by modifying the sensor without the need for analyte labeling.[3,5,6] Optical microdevices such as those based on highly sensitive whispering-gallery mode biosensors (WGMBs) have been developed to address the need for a sensitive and real-time tool in biodetection.[7–11] These microbead sensors have been applied to the detection of various biomarkers. For example, WGMBs have been employed for the detection of proteins,[3,12–18] DNA,[6,19,20] RNA[21] and virus particles.[7,10,22–24] The whispering-gallery mode biosensor (WGMB) is capable of ultrahigh sensitivity even down to single DNA molecules[5] or to observe the ions interactions.[25] Furthermore, label-free and real-time monitoring of cell apoptosis in cell cultures can be useful for developing organ-on-chip assays and to monitor and quantify the response of complex cell cultures exposed to various drugs and toxins.[3,26–28] To address the need for noninvasive and real-time tools capable of monitoring cell death, we developed a microfluidics integrated micrometer-scale optical biosensor that is capable of monitoring both cell morphology and specific biomarker.

Biomarkers are launched into the medium upon cell death due to exposure to staurosporine toxins, which are known to trigger apoptosis.[29] The shifts in the optical

Dr. Y.-J. Chen, U. Schoeler,[+] Prof. F. Vollmer[++]
Max Planck Institute for the Science of Light
91054 Erlangen, Germany
E-mail: ying-jen.chen@mpl.mpg.de; f.vollmer@exeter.ac.uk
Dr. Y.-J. Chen, U. Schoeler
Erlangen Graduate School in Advanced Optical Technology (SAOT)
Friedrich-Alexander Universität Erlangen-Nürnberg (FAU)
Paul-Gordan-Str. 6, D-91052 Erlangen, Germany
C.-H. (B.) Huang, Prof. F. Vollmer
Brigham & Women's Hospital
Harvard Medical School
Boston, MA 02115, USA
The ORCID identification number(s) for the author(s) of this article can be found under https://doi.org/10.1002/smll.201703705.
[+]Present address: Institute of Medical Biotechnology, Department of Chemical and Biological Engineering, Friedrich-Alexander-University Erlangen-Nürnberg (FAU), D-91052 Erlangen, Germany
[++]Present address: Living Systems Institute, Department of Physics and Astronomy, University of Exeter, Exeter EX4 4QD, UK

DOI: 10.1002/smll.201703705

resonance wavelength of a glass microsphere supporting WGMs[8,11,12,14,16,17,30] are used for tracking cytochrome c concentration for cell apoptosis assessment.[31] Note that the mechanism of extracellular cytochrome c is not well understood. The release of cytochrome c into extracellular space may indicate not only cell apoptosis, but also other unclear mechanisms such as cell signaling.[32] Extracellular cytochrome c has recently been used as biomarker for many apoptosis related diseases, such as arthritis.[33] or cancers.[34]

Cytochrome c is translocated from mitochondria to the cytoplasm and then into the cell culture medium during cell apoptosis.[35,36] Moreover, cytochrome c is also considered a useful biomarker for mitochondrial and general cellular damage.[37] There is also a relative abundance of cytochrome c within cells (i.e., estimated concentrations in intermembrane space between 0.5×10^{-3} and 5×10^{-3} M.[4]

Using WGMBs functionalized with cytochrome c-specific antibodies, we monitor the secretion of cytochrome c in real time after staurosporine treatment. Combining this with an imaging system, we are able to simultaneously monitor not only the release of biomarkers but also observe the morphology of the cells during the drug treatment. To functionalize the surface of the microbead, we applied a sandwich assay with the linking of biotin–streptavidin.[6] Antibodies are immobilized on the microbead sensor by conjugating the biotinylated antibody via streptavidin to a biotinylated dextran layer that was previously physisorbed to the glass microsphere. The biotinylated dextran layer efficiently prevents the nonspecific binding of substances contained in the complex medium to the WGMB.

Microfluidic devices provide control over a stable flow of analyte by increasing the mixing rate of different reagents and decreasing the volume of the sample,[38,39] gently and stably guiding it into the system. The microfluidic device is patterned with various sizes of blocks that act as filters or trappers. The blocker sizes are in the range of 5–50 μm. While the sample is flowing from larger to smaller filters, cells are being filtered according to their size thus allowing for size-dependent trapping. Here we use Jurkat cells that are sized within the range of 7–15 μm. The outlet of the device then introduces the medium into the optical sensing area. While the cells are being loaded onto the microfluidics device, the staurosporine is then pumped into the device and continuously flushes the cells trapped in the filters ($\approx 2 \times 10^4$ cells). In Jurkat cells, the mitochondria start to swell and release of cytochrome c has been observed within 1 h of staurosporine treatment.[40] The released cytochrome c proteins in the cell culture medium will bind to the antibody-functionalized WGMBs and lead to optical frequency shifts. The quantitative response of the WGMB to cell death is consistent with established cell viability MTT 3-(4,5-dimethylthiazol-2-yl)-2,5-diphenyltetrazolium bromide tests, i.e., the invasive colorimetric assay to monitor mitochondrial enzyme activities tied to relative cell viability.[33,41]

2. Results

2.1. Surface Functionalization

We applied the sandwich assay of biotin–streptavidin linking to immobilize the antibodies on the surface of the microbeads. The microbead is first modified by biotin–dextran, wherein dextran prevents nonspecific binding and the biotin links to the biotinylated antibody–streptavidin compound. **Figure 1**A

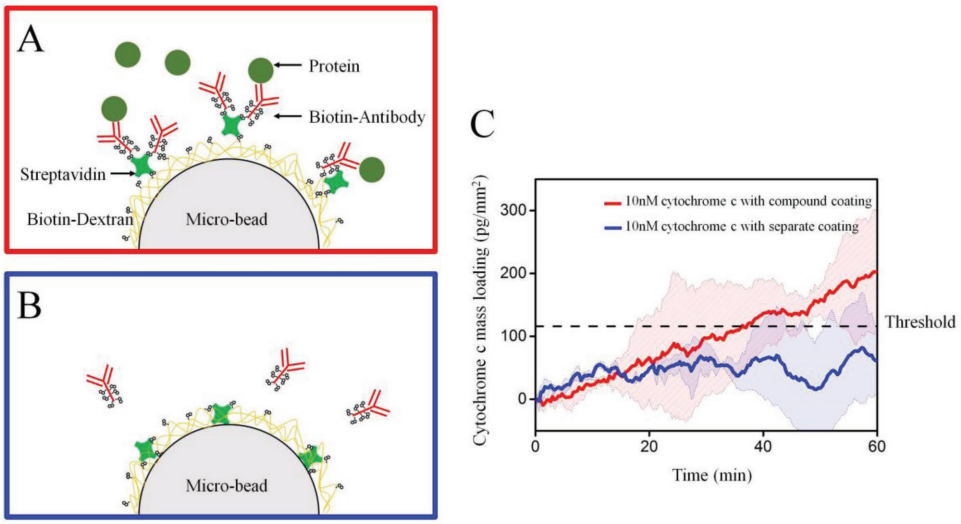

Figure 1. Surface modification with/without premixing of biotinylated antibody and streptavidin. A) Surface modification with biotinylated antibody and streptavidin premixing. The antibody is successfully immobilized on the microbead surface (red frame). B) Surface modification without biotinylated antibody and streptavidin premixing. The streptavidin is fully occupied by the biotins, which conjugated on the dextran chain. No free streptavidin binding sites are available for biotinylated antibody (blue frame). C) WGMB sensorgram of with and without premixing. 10×10^{-9} M human recombinant cytochrome c is used for testing. System threshold is determined by BSA nonspecific binding. Red curve indicates that cytochrome c binds to the microbead with premixing. Significant cytochrome c binding signal is observed. Blue curve indicates the microbead without premixing of biotinylated antibody and streptavidin. Streptavidin is first coated to the microbead. The streptavidin modified microbead is then exposed under biotinylated antibody solution. No significant cytochrome c binding is observed.

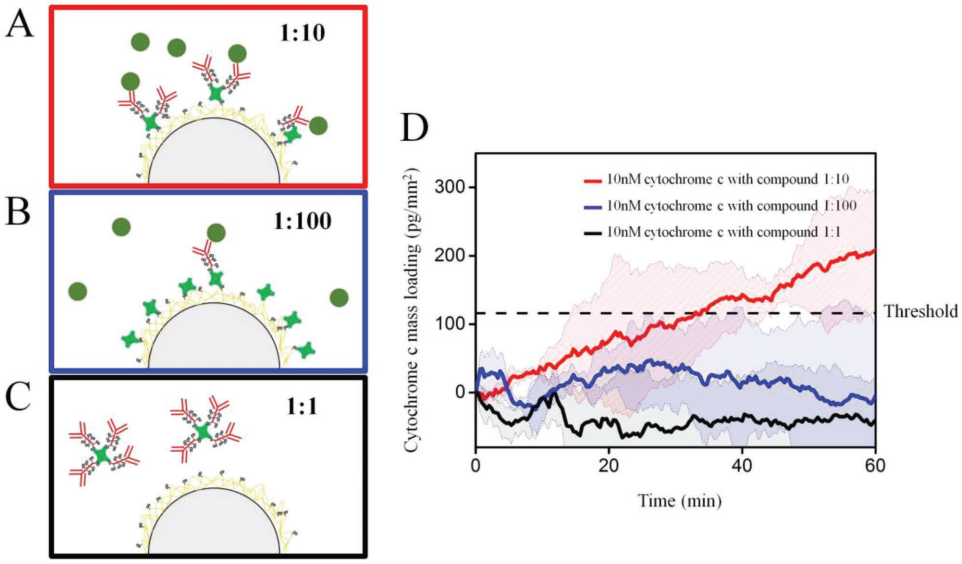

Figure 2. Surface functionalization with different compound ratio of biotinylated antibody and streptavidin. A) Compound of biotinylated antibody–streptavidin with mixing ratio 1:10 (red frame). Each streptavidin carries up to three biotinylated antibodies and link to the biotin on the microbead. Many cytochrome c proteins are bound to the functionalized microbead. B) Compound of biotinylated antibody–streptavidin with mixing ratio 1:100 (blue frame). Many free streptavidin bind to the microbead surface. Only few antibodies are immobilized on the microbead surface. C) Compound of biotinylated antibody–streptavidin with mixing ratio 1:1 (black frame). The streptavidin are fully occupied by the biotinylated antibodies and leave no free binding site to link to the biotins on the microbead surface. D) WGMB sensorgram of microbeads modified by three different mixing ratio compounds, respectively. 10×10^{-9} M human recombinant cytochrome c is used for testing. Threshold is determined by BSA nonspecific binding. Red curve indicates the cytochrome c binding of microbead functionalized by biotinylated antibody–streptavidin compound mixing with 1:10 ratio. Significant cytochrome c mass loading is observed. Blue curve indicates the cytochrome c binding of microbead functionalized by 1:100 compound ratio. Black curve indicates the cytochrome c binding of microbead functionalized by 1:1 compound ratio. No significant cytochrome c bindings are observed in both 1:100 and 1:1 compound.

displays the schematic for antibody immobilization. The surface of the microbead is modified with biotin–dextran, which provides two functions: first, it supplies the biotin linker necessary for linking to the biotinylated antibody–streptavidin compound and second, it minimizes the nonspecific adsorption of proteins to the glass microsphere surface. Mixing biotinylated antibody with streptavidin in advance is critical because it prevents the binding sites of streptavidin from being fully occupied by biotin–dextran on the surface of the microbeads. Figure 1B shows the schematic for unsuccessful surface modification if biotinylated antibody and streptavidin are not mixed in advance. After exposing the microspheres to biotinylated dextran they are first exposed to the streptavidin solution, and then exposed to the biotinylated antibody solution. The streptavidin is fully occupied by the biotin on the microbeads and hence there are no binding sites for linking to biotinylated antibody (Figure 1B). Figure 1C shows the cytochrome c binding with (red curve) and without premixing (blue curve) of biotinylated antibody and streptavidin. When the premixed compound was used (red curve), a significant amount of cytochrome c binds to the microbead, indicating that the antibodies are successfully immobilized on the microsphere surface. When separating the streptavidin and antibody coating step to two steps the WGMB data shows no significant cytochrome c binding (blue curve).

It is important to optimize the compound ratio between biotinylated antibody and streptavidin. It is desirable to immobilize as many antibodies as possible as to increase the WGMB signal; however, too many biotinylated antibodies may fully occupy the binding sites of streptavidin and prevent the compound from binding to the microbead. **Figure 2** displays the antibody immobilizing mechanisms with different conditions. Figure 2A displays the WGMB signal of recombinant human cytochrome c protein binds to the microbeads, which are functionalized by three different biotinylated antibody–streptavidin compounds respectively. Three different mixing ratios are tested with 10×10^{-9} M of cytochrome c. Figure 2D depicts the cytochrome c signal with three different ratios of compounds. The blue curve is for 1:100, black curve for 1:1, and red curve for 1:10 biotinylated antibody–streptavidin mixing ratios. Figure 2B (blue frame) displays the binding sketch for a compound ratio of 1:100. The WGMB signal (Figure 2D, blue curve) is low in this case. The low ratio between antibody and streptavidin ensures that there are free streptavidin binding sites for linking to the biotin on the microbead; however, the amount of antibodies that are immobilized on the microbead surface is insufficient. Figure 2C (black frame) displays the binding sketch for a compound ratio of 1:1. The WGMB signal (Figure 2D, black curve) shows weak cytochrome c binding. When the biotinylated antibody proportion is too high (i.e., a biotinylated antibody–streptavidin ratio 1:1), all the streptavidin binding sites are occupied by the biotinylated antibody, leaving no free binding site for the biotin on the surface of the microbead. Figure 2A (red frame) is for a compound ratio of 1:10. This shows a significant WGMB signal (Figure 2D, red curve) as compared to the other two compounds. Mixing biotinylated antibodies and streptavidin with a molecular ratio of 1:10 thus provides us with an optimized

sensing signal (Figure 2D, red curve). Approxmately 6 biotins are attached on each antibody to link with streptavidin.

2.2. Human Recombinant Cytochrome c WGMB Binding Signal

Figure 3 outlines the WGMB signal for recombinant cytochrome c in different concentrations. To understand the relationship between the signal generated by WGMBs and the concentration of cytochrome c, we use human recombinant cytochrome c protein (Novoprotein, CF80, USA) to calibrate the system. Figure 3 displays the sensor signals for four different concentrations of cytochrome c solution (30×10^{-9}, 20×10^{-9}, 10×10^{-9}, 0×10^{-9} M) in Tris buffer. All the measurements are repeated three times. Prior to cytochrome c injection, the sensor reaches thermal equilibrium at room temperature for 30 min and a baseline is recorded for more than 5 min. There is no significant baseline drift and the WGM wavelength shift noise levels are at ±0.04 pm, corresponding to an uncertainty of ±4 pg mm^{-2} when determining mass loading. Recombinant cytochrome c protein binds to the antibody on the microbead and causes the wavelength shift. The wavelength shift is translated into cytochrome c mass loading (see the Experimental Section). Figure 3 inset shows the WGM sensorgram and the binding slope of these four concentrations. The binding slope (Figure 3 inset) is determined by first 30 min of the measurement (see the Supporting Information). The specificity of the microbead is tested by high concentration of bovine serum albumin (BSA), which is commonly used in biological experiments to block the nonspecific binding. The WGM signal generates from BSA (Figure 3, orange curve) is considered as the background of nonspecific binding and set as the threshold of sensor (see the Experimental Section for details). The threshold is determined by the first 30 min of the BSA binding, which is 2.04 pg mm^{-2} min^{-1}.

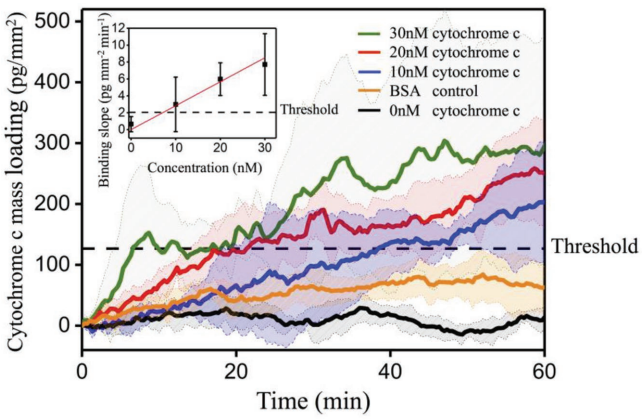

Figure 3. System calibration by human recombinant cytochrome c protein. The sensorgram of 1×10^{-6} M BSA control and four different cytochrome c dilution. Four different concentrations are measured to abstract calibration curve. 30×10^{-9} M (green curve), 20×10^{-9} M (red curve), 10×10^{-9} M (blue curve), and 0×10^{-9} M (black curve) of cytochrome c solution are measured. Orange curve is the system response to 1×10^{-6} M of BSA solution. The average of nonspecific mass loading plus standard deviation is used to determine the system threshold. Signal under threshold is considered as a background signal. Inset figure shows the initial binding slope of these concentrations. Initial binding slope is proportional to the cytochrome c concentration. Threshold is determined by the first 30 min of 1×10^{-6} M BSA binding.

2.3. Real-Time Cytochrome c Detection from Jurkat Cells

Figure 4 contains the real-time measurement of cytochrome c released from the Jurkat cells after staurosporine treatment. All experiments are repeated three times and the index change caused by staurosporine injection is compensated (see the Supporting Information). The experiment is operated in room temperature. The red curve represents the Jurkat cells treated by 1×10^{-6} M staurosporine while the dark blue curve represents the cells that have not been treated. The brown curve encompasses the control measurement without Jurkat cells. The microbead is immersed in the cell culture medium to block the nonspecific binding sites for ≈1 h and the baseline is recorded for more than 5 min. A significant amount of cytochrome c is detected after 2 h of staurosporine treatment. Approxmately 5.4 pmol of cytochrome c is released within first 2 h after staurosporine treatment. Each cell releases sub-fmol (≈0.27 fmol) of cytochrome c to the surrounding medium. The amount of cytochrome c release is estimated by the interpolation of calibration curve as given in Figure 3. Figure 4 inset depicts the cell viability determined by MTT assay that is a commonly used for quantitative monitoring of mitochondrial enzyme activity. The MTT assay is a high throughput homogeneous cell viability assay.[42] and the MTT reagent is positively charged and able to penetrate the cells. Viable cells will convert MTT into purple colored formazan. By contrast, dead cells will have lost

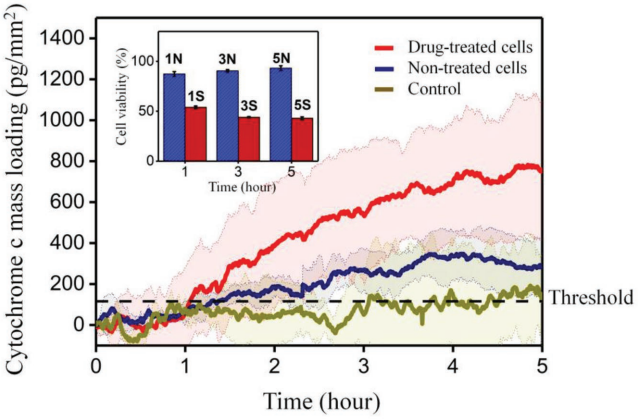

Figure 4. Real-time sensing of cytochrome c released from Jurkat cells. Brown curve indicates the control measurement of only serum free medium without cells. The result validates the system stability for long-term measurement. Dark blue curve indicates the Jurkat cells without staurosporine treatment. Small amount of cytochrome c is observed within 5 h of measurement. Red curve indicates Jukat cells treated by 1×10^{-6} M staurosporine. Significant WGM signal is observed. Inset figure indicates cell viability determined by MTT assay with/without staurosporine treatment. Blue bars (1N, 3N, 5N) indicate the cell viability of Jurkat cells in room temperature without staurosporine treatment. Result shows no significant decrease of cell viability after 5 h located in room temperature. Red bars (1S, 3S, 5S) indicate the Jurkat cells viability after 1×10^{-6} M staurosporine treatment. The cell viability is decreasing with longer treating time.

Table 1. Jurkat cells treating condition for MTT assay.

Sample	Time point [h]	Treatment condition
0B	0	No cells, no treatment
0C	0	With cells, no treatment
1N	1	With cells, no treatment
1S	1	With cells, staurosporine treated
3N	3	With cells, no treatment
3S	3	With cells, staurosporine treated
5N	5	With cells, no treatment
5S	5	With cells, staurosporine treated

the ability to convert MTT into purple color. The amount of the formazan is generally proportional to the number of metabolically active viable cells.[43]

Different time points (0 h, 1 h, 3 h, 5 h) are measured to determine the cell viability. All the experiments are repeated for three times, and the shown graph is the mean value of the experiments with standard deviation as error bar. The sample well without cells 0B (see **Table 1**) is set as the baseline that the absorption is only from MTT and serum free medium. The cells without treatment in 0 h (0C) is used for normalization. The MTT results show that the cell viability of the cells without treatment (Figure 4 inset blue bars, sample 1N, 3N, 5N) are quite stable in room temperature. The cell viability of the staurosporine treated samples (Figure 4 inset red bars, sample 1S, 3S, 5S) are gradually decreasing, which are inversely proportional to the staurosporine incubation time.

3. Discussions and Conclusions

In this paper, we developed a highly sensitivity, label-free, noninvasive, microfluidics integrated WGMB platform for the real-time detection of a biomarker released from cells. The amount of cytochrome c released by Jurkat cells into the medium was quantified to draw conclusions regarding cell viability in response to staurosporine treatments.

Compared to current protein analytical tools such as ELISA assay, which requires protein labeling,[44,45] the WGM-based optical platform demonstrated in this research provides a label-free, highly sensitive and real-time approach to detect specific biomarkers in the medium. The capability of real-time, extracellular detection provides a novel tool to monitor the specific secretion of biomarkers by live cells after drug treatment. By contrast, other existing methods used to analyze specific biomarkers of cells such as ELISA or Western Blot require lysing of the cells or labeling of the protein. Such approaches either prevent real-time observation of cell response or result in a nonphysiological condition of cells due to the labeling procedure.

We also presented a surface functionalization method to detect a specific protein in a complex media. This WGMB platform is adaptable for detection of virtually any biomarker via antibody-based recognition schemes.

In this study, we applied monoclonal cytochrome c antibodies for specific detection. In order to reduce nonspecific binding in a complex medium we modified the sensor surface with a biotin-dextran layer.[3,6,46] The functionalized microbead is tested with a high concentration of BSA to determine a concentration threshold above which the sensor response can be mainly attributed to specific binding. The detection limit of cytochrome c in complex media is 6.82×10^{-9} M, which is determined by 1 μm of BSA solution.

We monitored a significant amount of cytochrome c that was released into cell culture medium after staurosporine treatment as shown in Figure 4, red curve. Meanwhile, the MTT assay also shows the decrement of cell viability. Note that the results from MTT assay and WGMB are not directly comparable. Staurosporine could induce cell apoptosis[29] and cell cycle arrest,[47] both aspects of which may influence the MTT result. A release of cytochrome c into extracellular space after triggering cell apoptosis was reported.[35] However, recent research has found that the releasing of cytochrome c into extracellular space may have different functions such as intracellular signaling molecule of the brain.[32] The mechanism for extracellular cytochrome c release is not well understood, and so to draw any concrete conclusion further studies are required. The platform demonstrated in this work provides a novel approach for scientists to monitor the real-time response of a cell to drug treatment.

The integration of WGMBs with a microfluidics system that continuously delivered fresh cell culture media furthermore allowed for the precise control over the dose of a drug administered during biosensor measurements. This microfluidic WGMB platform represents a potentially powerful tool for analyzing the response of cells in various microenvironments, in real time and without the need for cell lysis. The biochip detection system could be easily integrated with other bioanalytical platforms such as confocal microscopy in order to simultaneously monitor morphological changes of cells or the re-distribution of fluorescently labeled proteins expressed inside of the cells. Various microfluidics integrated WGMB devices could provide a multiplexed platform for researchers to quantitate proteins released by cells for example in applications that seek to optimize protein or antibody production or that seek to understand the complex response kinetics of cells or that study the secretome.

Meanwhile, by modifying the microfluidic device further, small amounts of protein secreted from tissue samples after drug treatment could be collected and analyzed without inflicting any damage to the tissue; and ultrasensitive WGMBs are potentially capable of monitoring the single cell response possibly down to the single molecule level. With the further improvement of the microfluidic WGMB technology, one could culture cells[48,49] and tissues on 3D[50,51] scaffolds that integrate WGMBs to monitor the specific release of biomarkers within a complex organ-on-a-chip and at different sensing locations within the scaffold.

4. Experimental Section

System Schematic, Microbead Fabrication, and Functionalization: **Figure 5**A displays the system schematic. The evanescent field is coupled into the microbead via a prism coupling setup. The laser wavelength is 1310 nm, the refractive index of the prism (Edmund, N-SF11) is 1.748, and the incident beam angle is ≈55°. The solution is continuously pumped through the cell trapper and flows into the sensing area via syringe pump driven pressure (Harvard Apparatus 11 Plus, USA) for

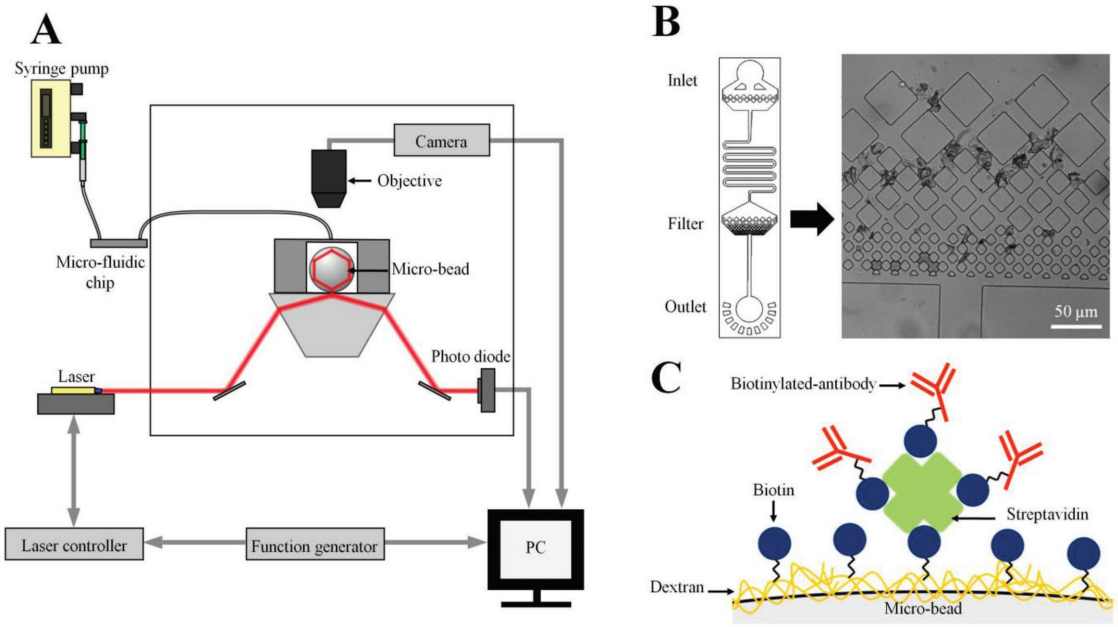

Figure 5. Microfluidic integrated WGMB. A) WGMB system schematic. The solution continuously pumped into the microfluidic chip where the cells are located, with a consistent flowrate in which the solution contains analytes is launched in the sensing chamber. The analyte is specifically captured by antibody functionalized microbeads. The WGMB signal is acquired by a DAQ card and analyze by a PC. B) Left: Microfluidic chip. The cells are launched from the inlet and been trapped in the filter. The filter contains variety sizes of blockers to trap the cells. The curving channel design efficiently reduces the noise generates by syringe pump, which may cause inconsistency of the flowrate. Right: The Jurkat cells trapped in the microfluidic device. C) Illustration of surface functionalization. The microbead is modified by anticytochrome c antibodies via sandwich assay of streptavidin–biotin binding. The microbead is first modified a biotin–dextran layer (yellow chains). The compound of biotin–antibody and streptavidin is then modified. The streptavidin binds biotin on surface of the microbead and the biotinylated antibody.

uninterrupted measurement. The drug keeps flushing the cells, and the antigen is captured by the surface functionalized microbead. Figure 5B left shows the design of the microfluidic chip. The solution is injected from the inlet, passing through the curving channel, which is designed to stabilize flowing media cause by syringe pump regular pulses and delivered to the area where the cells are trapped. The cell trapping region contains filter patterns sizing from 5 to 50 μm and it was designed to capture cells sizing from 7 to 15 μm. Figure 5B right shows the image of cell trapping via bright-field microscopy. In the end, the solution that contains protein that releases from captured cells flow out of the device and reach to the sensing area. The microfluidics chip is connected to the sensing chamber by a 0.381 mm ID and 1.09 mm OD polyethylene tube. Figure 5C shows the illustration of surface modification. Streptavidin plays the role as bridge to link the biotin on the microbead surface and the biotinylated antibody.

Microbead Fabrication: The microbead is fabricated using a single mode fiber with a 250 μm acrylate polymer coating and 125 μm of cladding. After the jacket is removed, the exposed fiber is cleaned with acetone and isopropanol to remove the acrylate residue. The fiber is then melted by oxygen–butane flame with ≈3000 °C (estimated by the color) under a microtorch. The microbead is observed by a microscope to ensure the spherical of the shape.

Surface Modification: The antibodies are immobilized on the surface of the microbead by a sandwich assay of biotin–streptavidin. The microbeads were first placed in a plasma cleaner (Harrick Plasma, Basic Plasma Cleaner PDC-32G, USA) for 5 min to undergo surface hydroxylation. After plasma treatment, the microbead was exposed to biotin–dextran solution (Sigma-Aldrich, 14402, Germany) for 30 min. After the biotin–dextran treatment, the microbeads were washed three times with Tris buffer, each washing duration being 5 min as to remove the free biotin–dextran solution. Next, the microbeads were exposed to a premixed solution of biotinylated antibodies and streptavidin for 1 h. The biotinylated antibody–streptavidin compound was prepared 24 h before the experiments with an optimized molecular stoichiometric concentration ratio of 10:1 (see Section 2). The anticytochrome c antibodies (Biolegend, 612303) were premodified with ≈3–6 molecules of biotin per antibody. Efficient linkage of the biotinylated antibody to streptavidin (New England Biolabs, N7021S, England) ideally requires 2–3 binding sites of streptavidin occupied by the antibody, leaving 1–2 binding sites for linkage to the biotinylated dextran layer.

WGMB Data Analysis: The microoptical resonance wavelength shift of the WGMB upon cytochrome c protein binding is measured in units of loaded protein mass per millimeter squared sensor area (pg mm^{-2})[6]

$$\text{Mass loading} = \frac{\Delta\lambda}{\lambda}\frac{\left(n_s^2 - n_m^2\right)R}{2n_m\left(dn/dc\right)} \quad (1)$$

where $\Delta\lambda$ is the shift in the resonance wavelength, λ is the nominal wavelength of the distributed feedback laser (DFB) laser (≈1310 nm), $n_s = 1.46$, and $n_m = 1.33$ are the respective refractive indices of the microsphere and aqueous medium, R is the approximate radius of the microsphere as determined by microscopic imaging (≈200 μm), and $dn/dc \approx 0.183 \times 10^{-9}$ (mm^3 pg^{-1}) is the approximate incremental refractive index change of a cytochrome c protein solution.[30]

Microfluidic Device: The microfluidic device used to trap the cells is a device with a glass slide and patterned polydimethylsiloxane (PDMS) leaf bonded chip. The devices are roughly 3 mm thick, 76.2 mm long, and 50.8 mm wide as shown in Figure 5B. The height of the channel is 50 μm and the width of the curving channel is 30 μm (Figure 5B). The channel was molded by a microfabricated SU-8 3025 master on a silicon wafer followed by PDMS soft lithography. The PDMS leaf was released after 3 h of 85 °C curing in the oven. After hole punching the inlet and outlet, the PDMS leaf was rinsed with isopropyl alcohol and dried out with compressed N_2 gas. To fully dehydrate the PDMS leaf, the leaf was baked in the oven at 85 °C for 10 min. PDMS leaves were then O_2 plasma-treated with acetone-cleaned glass slides. The device was then finalized via PDMS and glass slide bonding. An optional 10 min postbinding bake at 85 °C in the oven helped minimize vapor or any

liquid leftover at the binding interface, thus strengthening the binding. The devices were tape-sealed until usage as to avoid introducing unwanted particles or dirt contamination. Note that 0.381 mm ID and 1.09 mm OD polyethylene tubing was used to connect the flow-through device and optical system.

Cell Preparation: The cells were maintained in RPMI-1640 medium (Gibco, Life Technologies) supplemented with 10% heat-inactivated fetal calf serum (FCS HI, Sigma) and 1% penicillin–streptomycin–glutamine (PSG, Invitrogen) at 37 °C in 5% CO_2. Before the experiments the cells were first washed and then transferred to serum-free RPMI-1640 medium supplemented with 1% PSG. For this cleaning procedure, 10 mL of cell suspension was transferred to a 15 mL tube and centrifuged for 5 min at 1200 rpm. The supernatant was discarded, and the cells were resuspended in 14 mL of Dulbecco's phosphate buffered saline (DPBS, Gibco), and, again, centrifuged for 5 min at 1200 rpm. The washing step was repeated and after that, the DPBS supernatant was discarded and the cells were resuspended in 10 mL of serum-free medium supplemented with 1% PSG. The cell numbers were determined by a counting chamber. For the WGMB experiments the cell solution was further diluted to a cell density of 4×10^4 cells mL^{-1}. 500 µL of this dilution (i.e., 2×10^4 cells) were flowed through the microfluidic system.

MTT Assays: MTT 3-(4,5-dimethylthiazol-2-yl)-2,5-diphenyltetrazolium assays are applied to validate the cell viability with and without staurosporine treatment (Sigma-Aldrich, S6942-200UL) at room temperature. The Jurkat cells were cultured for 2 d and replaced to serum free medium before the experiment (see *Cell Preparation*). To mimic the sealed environment for microfluidic system, 10^5 of Jurkat cells were loaded into polymerase chain reaction (PCR) tubes, each contained 100 µL of serum-free medium. The tube was sealed after the treatment to remain CO_2 level and kept pH of the cell culture medium stable. The cell viability was monitored in various time points as Table 1. 5N (staurosporine free) and 5S were treated first and sealed the PCR tubes. After 2 h, the experiments of 3N and 3S were started. The samples were prepared in order, and in the end, all tubes were opened at the same time and the cells were moved to the 96-well plate. In the meantime, 10 µL of MTT solution was added to each well. The 96-well plates were incubated under 37 °C overnight. After incubation, 10 µL of SDS/HCl was added into each well to dissolve the formazan crystals.[43,52] The formazan was observed with 550 nm to get the optical density.

Supporting Information

Supporting Information is available from the Wiley Online Library or from the author.

Acknowledgements

F.V. would like to acknowledge financial support through NIH R01 Grant No. 1R01GM095906-01 from the National Institute of General Medical Sciences, USA, as well as funding from the Max Planck Society, Germany, and the funding provided by the University of Exeter. All authors would like to express their gratitude to Prof. Ben Fabry, Prof. Joseph V. Bonventre for supplying cells and the culturing facilities, Prof. David A. Weitz for providing cells and microfluidics facility, Prof. Slany for his guidance on experiments with MTT assays, Martin Baaske and Sivaraman Subramanian for advising on the prism coupling technique, Xiao Xia Zhong for assistance with MTT assays, Astrid Mainka for technical support, and Serge Vincent for his assistance with manuscript revisions.

Conflict of Interest

The authors declare no conflict of interest.

Keywords

apoptosis, cytochrome c, microfluidics, MTT assay, optofluidics, surface functionalization, whispering-gallery mode biosensor

Received: October 24, 2017
Revised: March 10, 2018
Published online:

[1] S. W. Lowe, A. W. Lin, *Carcinogenesis* **2000**, *21*, 485.
[2] N. Ke, X. Wang, X. Xu, Y. A. Abassi, *Methods Mol. Biol.* **2011**, *740*, 33.
[3] Y.-J. Chen, W. Xiang, J. Klucken, F. Vollmer, *Nanotechnology* **2016**, *27*, 164001.
[4] N. J. Waterhouse, J. A. Trapani, *Cell Death Differ.* **2003**, *10*, 853.
[5] M. D. Baaske, M. R. Foreman, F. Vollmer, *Nat. Nanotechnol.* **2014**, *9*, 933.
[6] Y. Wu, D. Y. Zhang, P. Yin, F. Vollmer, *Small* **2014**, *10*, 2067.
[7] F. Vollmer, S. Arnold, D. Keng, *Proc. Natl. Acad. Sci. USA* **2008**, *105*, 20701.
[8] A. L. Washburn, L. C. Gunn, R. C. Bailey, *Anal. Chem.* **2009**, *81*, 9499.
[9] H. A. Huckabay, R. C. Dunn, *Sens. Actuators, B* **2011**, *160*, 1262.
[10] T. Lu, H. Lee, T. Chen, S. Herchak, J.-H. Kim, S. E. Fraser, R. C. Flagan, K. Vahala, *Proc. Natl. Acad. Sci. USA* **2011**, *108*, 5976.
[11] C. E. Soteropulos, K. M. Zurick, M. T. Bernards, H. K. Hunt, *Langmuir* **2012**, *28*, 15743.
[12] J. T. Gohring, P. S. Dale, X. Fan, *Sens. Actuators, B* **2010**, *146*, 226.
[13] M. S. Luchansky, R. C. Bailey, *Anal. Chem.* **2010**, *82*, 1975.
[14] M. S. Luchansky, R. C. Bailey, *J. Am. Chem. Soc.* **2011**, *133*, 20500.
[15] C. Delezoide, M. Salsac, J. Lautru, H. Leh, C. Nogues, J. Zyss, M. Buckle, I. Ledoux-Rak, C. T. Nguyen, *IEEE Photonics Technol. Lett.* **2012**, *24*, 270.
[16] K. A. Wilson, C. A. Finch, P. Anderson, F. Vollmer, J. J. Hickman, *Biomaterials* **2012**, *33*, 225.
[17] K. A. Wilson, C. A. Finch, P. Anderson, F. Vollmer, J. J. Hickman, *Biomaterials* **2015**, *38*, 86.
[18] H. A. Huckabay, S. M. Wildgen, R. C. Dunn, *Biosens. Bioelectron.* **2013**, *45*, 223.
[19] J. D. Suter, I. M. White, H. Zhu, H. Shi, C. W. Caldwell, X. Fan, *Biosens. Bioelectron.* **2008**, *23*, 1003.
[20] F. Wu, Y. Wu, Z. Niu, F. Vollmer, *Sensors* **2016**, *16*, 1197.
[21] O. Scheler, J. T. Kindt, A. J. Qavi, L. Kaplinski, B. Glynn, T. Barry, A. Kurg, R. C. Bailey, *Biosens. Bioelectron.* **2012**, *36*, 56.
[22] L. He, S. K. Ozdemir, J. Zhu, W. Kim, L. Yang, *Nat. Nanotechnol.* **2011**, *6*, 428.
[23] V. R. Dantham, S. Holler, V. Kolchenko, Z. Wan, S. Arnold, *Appl. Phys. Lett.* **2012**, *101*, 043704.
[24] L. Shao, X.-F. Jiang, X.-C. Yu, B.-B. Li, W. R. Clements, F. Vollmer, W. Wang, Y.-F. Xiao, Q. Gong, *Adv. Mater.* **2013**, *25*, 5616.
[25] M. D. Baaske, F. Vollmer, *Nat. Photonics* **2016**, *10*, 733.
[26] S. N. Bhatia, D. E. Ingber, *Nat. Biotechnol.* **2014**, *32*, 760.
[27] A. Polini, L. Prodanov, N. S. Bhise, V. Manoharan, M. R. Dokmeci, A. Khademhosseini, *Expert Opin. Drug Discovery* **2014**, *9*, 335.
[28] F. An, Y. Qu, X. Liu, R. Zhong, Y. Luo, *Anal. Chem. Insights* **2015**, *10*, ACI.S28905.
[29] R. Bertrand, E. Solary, P. O'Connor, K. W. Kohn, Y. Pommier, *Exp. Cell Res.* **1994**, *211*, 314.
[30] M. R. Foreman, J. D. Swaim, F. Vollmer, *Adv. Opt. Photonics* **2015**, *7*, 168.
[31] C. M. Luetjens, D. Kögel, C. Reimertz, H. Düßmann, A. Renz, K. Schulze-Osthoff, A.-L. Nieminen, M. Poppe, J. H. M. Prehn, *Mol. Pharmacol.* **2001**, *60*, 1008.

[32] A. Gouveia, E. Bajwa, A. Klegeris, *Biochim. Biophys. Acta, Gen. Subj.* **2017**, *1861*, 2274.
[33] M. V. Berridge, P. M. Herst, A. S. Tan, *Biotechnol. Annu. Rev.* **2005**, *11*, 127.
[34] J. Javid, R. Mir, P. K. Julka, P. C. Ray, A. Saxena, *Tumor Biol.* **2015**, *36*, 4253.
[35] A. Renz, W. E. Berdel, M. Kreuter, C. Belka, K. Schulze-Osthoff, M. Los, *Blood* **2001**, *98*, 1542.
[36] B. Ahlemeyer, S. Klumpp, J. Krieglstein, *Brain Res.* **2002**, *934*, 107.
[37] T. Eleftheriadis, G. Pissas, V. Liakopoulos, I. Stefanidis, *Front. Immunol.* **2016**, *7*, 279.
[38] S. A. N. Gowers, V. F. Curto, C. A. Seneci, C. Wang, S. Anastasova, P. Vadgama, G.-Z. Yang, M. G. Boutelle, *Anal. Chem.* **2015**, *87*, 7763.
[39] G. Luka, A. Ahmadi, H. Najjaran, E. Alocilja, M. DeRosa, K. Wolthers, A. Malki, H. Aziz, A. Althani, M. Hoorfar, *Sensors* **2015**, *15*, 30011.
[40] J. L. Scarlett, P. W. Sheard, G. Hughes, E. C. Ledgerwood, H.-H. Ku, M. P. Murphy, *FEBS Lett.* **2000**, *475*, 267.
[41] F. Denizot, R. Lang, *J. Immunol. Methods* **1986**, *89*, 271.
[42] T. Mosmann, *J. Immunol. Methods* **1983**, *65*, 55.
[43] T. L. Riss, A. L. Niles, L. Minor, *The National Center for Advancing Translational Sciences*, Eli Lilly & Company **2004**, PMID 23805433.
[44] S. X. Leng, J. E. McElhaney, J. D. Walston, D. Xie, N. S. Fedarko, G. A. Kuchel, *J. Gerontol., Ser. A* **2008**, *63*, 879.
[45] E. Engvall, P. Perlmann, *Immunochemistry* **1971**, *8*, 871.
[46] J. Piehler, A. Brecht, K. Hehl, G. Gauglitz, *Colloids Surf., B* **1999**, *13*, 325.
[47] S. Bruno, B. Ardelt, J. S. Skierski, F. Traganos, Z. Darzynkiewicz, *Cancer Res.* **1992**, *52*, 470.
[48] M. Tehranirokh, A. Z. Kouzani, P. S. Francis, J. R. Kanwar, *Biomicrofluidics* **2013**, *7*, 051502.
[49] S. Halldorsson, E. Lucumi, R. Gómez-Sjöberg, R. M. T. Fleming, *Biosens. Bioelectron.* **2015**, *63*, 218.
[50] X. (James) Li, A. V. Valadez, P. Zuo, Z. Nie, *Bioanalysis* **2012**, *4*, 1509.
[51] V. van Duinen, S. J. Trietsch, J. Joore, P. Vulto, T. Hankemeier, *Curr. Opin. Biotechnol.* **2015**, *35*, 118.
[52] M. P. Garcia-Cuellar, J. Steger, E. Füller, K. Hetzner, R. K. Slany, *Haematologica* **2015**, *100*, 905.